3 Demethanization of aqueous anaerobic effluents using a
4 polydimethylsiloxane membrane module: mass transfer,
5 fouling and feasibility

6 M. Henares, M. Izquierdo, P. Marzal, and V. Martínez-Soria*
7 *Research Group GI²AM, Department of Chemical Engineering, University of Valencia,*
8 *Avda. Universitat s/n, 46100 Burjassot, Spain*
9 *Corresponding author: E-mail address: vmsoria@uv.es (V. Martínez-Soria)
10

11 Abstract

12 The performance, fouling and feasibility of a polydimethylsiloxane hollow fibre
13 membrane module for in situ methane degasification from the effluent of an Expanded
14 Granular Sludge Bed anaerobic reactor has been investigated. Experiments at different
15 operational conditions were carried out (liquid flow, sweep gas flow and vacuum
16 pressure) with maximum removal efficiency (77%) at lowest flow-rate (0.4 L h^{-1}),
17 highest vacuum (800 mbar) and liquid flowing in lumen side. Mass transport analysis
18 denoted a considerably higher methane transfer than that predicted (attributed to liquid
19 oversaturation). An enhancement factor for liquid phase has been proposed to
20 correlate the experimental results. Long-term experiments were also performed in
21 order to determine the possible influence of fouling on the module performance, and it
22 showed that relatively frequent cleaning with water might be carried out to ensure
23 preservation of the membrane efficiency. Although energy balance analysis evidenced
24 that energy production exceeded the system energy requirements, the economic profit
25 of the process does not seem fully-guaranteed. A substantial reduction of CO_2
26 equivalent emissions showed the positive environmental impact of this technology.

27

28 Keywords

29 Anaerobic reactor; methane degassing; membrane fouling; membrane contactor; mass
30 transfer

31

1. Introduction

The minimization of the loss of residual methane from aqueous effluents of anaerobically treated wastewater systems has recently attracted growing interest, with an increasing number of studies about it in the last years [1–4]. This interest is based on the fact that the recovery of this residual dissolved methane (or at least its removal) in these effluents presents several potential benefits of a diverse nature: environmental (avoiding the emission of a powerful greenhouse gas), economic (recovering a power source) and safety (reducing the possibility of creating an explosive atmosphere).

In addition, it has been frequently described [4–9] that dissolved methane can be found in these effluents in concentrations above the saturation level, which would suggest that the impact of the discharge of this residual methane may be even higher than expected, especially taking into account that more sustainable anaerobic processes should be carried out at relatively low-temperature [8], ambient or psychrophilic conditions (<20 °C), which favours the solubility of methane in water.

The development and implementation of a technology to economically recover dissolved methane from process effluents could improve the viability and sustainability of anaerobic wastewater treatment [1,4]. In this sense, the membrane hollow fibre contactor has emerged recently as a promising technology that seems able to demethanize aqueous streams, with benefits with respect to conventional separation technologies. Among such benefits are higher volumetric mass transfer coefficients that lead to compact and smaller systems [9] and avoiding the direct contact of liquid and gas phases that can frequently lead to problems such as foaming, flooding, and emulsions [10,11]. So, Bandara et al. [12–14] demonstrated that degasification using a multi-layered composite hollow fibre degassing module (with porous and non-porous materials) is a promising technology for improving methane recovery from the effluent of a bench-scale Upflow Anaerobic Sludge Blanket (UASB) process for treating low-strength wastewater at low temperature. In a preliminary work, Cookney et al. [6] showed the potential for recovering dissolved methane from low-temperature UASB treating domestic wastewater using a polydimethylsiloxane (PDMS) membrane contactor. This work was continued later by including a polypropylene microporous membrane contactor, and both synthetic and real anaerobic effluents form the UASB and membrane bioreactor [15]. The authors also showed that this application could both be economically practicable and avoid net CO_2 emissions. Luo et al. [16] demonstrated that a degassing membrane coupled UASB reactor was able to achieve in situ biogas upgrading and decrease the dissolved CH_4 concentration in the anaerobic effluent. Unfortunately, studies on the removal of residual dissolved methane from anaerobic effluents are still very scarce, and further research in this field is needed to improve and deepen the knowledge and performance of this technology, especially in that related to membrane fouling and long-term experiments.

In this context, research for in situ removal/recovery of methane from the effluent of an Expanded Granular Sludge Bed (EGSB) anaerobic reactor is being carried out in our research group. A comparative study of two different degassing membrane contactors [17], microporous (polypropylene) and non-porous (PDMS), showed that the performance of both contactors was not very unequal, but wetting phenomena were observed for the microporous module, which is one of the major potential bottlenecks

2

77 of this type of microporous material. In this sense, dense (or non-porous) membrane
78 materials can offer a solution to prevent wetting and may simultaneously offer
79 acceptable mass transfer performances [18].

80 In the first part of the present work we have extended our previous study [17] with
81 different operating conditions on the performance of the PDMS module for methane
82 degassing. An analysis of the experimental results based on a resistance to mass
83 transfer study is presented. In addition, and as especial novelty, the incidence of
84 membrane fouling in long-term experiments has been determined. To the best of our
85 knowledge, this is the first attempt in the literature to study the membrane fouling in
86 long term experiments in methane degassing of anaerobic effluents. Finally, a
87 feasibility study considering energy recovery and demand has been carried out for a
88 given application of a degassing process using a contactor of nonporous membrane of
89 PDMS.

90

91 **2. MATERIALS AND METHODS**

92 *2.1 Experimental set-up*

93   A commercial hollow fibre membrane contactor module (PDMSXA-250, supplied
94 by PermSelect®, MedArray Inc., USA) was selected as usual in water degassing
95 industrial applications. The main properties of the degassing module (DM) are
96 summarized in Table 1.

97

98   **Table 1**. Characteristics of the non-porous polydimethylsiloxane (PDMS) contactor
99   module.

Module inner diameter, m	0.016
Module length, m	0.14
Number of fibres	320
Effective fibre length, m	0.083
Inner diameter, µm	190
Outer diameter, µm	300
Fibre wall thickness, µm	55
Inner area (A_i), m^2	0.0159
Outer area (A_o), m^2	0.0250
Shell tube inner diameter, m	0.016
Packing fraction	0.113
Max. liquid flow rate L h^{-1}	12
Typical sweep gas flow rate, L h^{-1}	2.7-27.0
Lumen side volume, m^3	$7.53 \ 10^{-7}$
Shell side volume, m^3	$1.48 \ 10^{-5}$

|	
Max. shell to lumen TMP*, mbar	1050
Max. lumen to shell TMP*, mbar	3100

100 *TMP: Transmembrane pressure.

101 A laboratory scale EGSB anaerobic reactor was operated at 25 °C for almost 3 years.
102 The EGSB reactor was initially inoculated with 4 L of granular anaerobic sludge from
103 the wastewater treatment plant of a local brewery. The bioreactor treated 8 L d^{-1} of a
104 synthetic wastewater polluted with ethanol with an organic load rate of 32 kg chemical
105 oxygen demand (COD) m^{-3} d^{-1}, being a relatively high strength wastewater comparing
106 with most of conventional anaerobic treatments [4]. A high recirculation flow was
107 maintained to expand the sludge bed with an up-flow velocity of 10.7 m h^{-1}. A liquid–
108 gas separator device was placed at the top of the reactor, and the biogas was collected
109 through a sodium hydroxide solution. The methane flow rate and biogas composition
110 were monitored with a flow meter (MGC-10 PMMA, Ritter, Germany) and a biogas
111 analyser (Combimass GA-m, Binder, Germany), respectively. Water characteristics
112 based on pH, conductivity, alkalinity, volatile fatty acids, COD, solids and nutrients
113 concentrations were periodically checked. A detailed description of the biological
114 system and procedure can be found elsewhere [19].

115 A diagram of the EGSB reactor and the DM contactor is shown in Fig. 1. The
116 membrane module was coupled to the EGSB reactor and fed with a fraction of flow
117 from the recirculation stream, in which the concentration of the dissolved methane (D-
118 CH$_4$) was similar to that in the effluent stream. The stream was flowed and then
119 through the contactor, using a peristaltic pump (Watson-Marlow, USA), resulting in flow
120 rates from 0.4 to 10.8 L h^{-1}. A stainless-steel filter of 40 µm was set-up prior to
121 membrane module to avoid DM contactor clogging by the solid particulates from the
122 anaerobic reactor. This filter was periodically cleaned and no biofilm development was
123 observed on it. The liquid pressure drop at the inlet and outlet of the membrane was
124 measured using a portable manometer MP 112 (Kimo, Spain). For vacuum pressure
125 experiments, a vacuum pump N026.3.AT.18 (KNF Neuberger, Germany) was used for
126 vacuum operation, getting vacuum pressures (P_{vac}) of 140, 500 and 800 mbar. For
127 countercurrent sweep gas experiments, nitrogen gas with a high purity (> 99.8%)
128 supplied by Carburos Metálicos S.A. (Spain) was introduced into the contactor with
129 flow rates ranging between 2.7 and 27.0 L h^{-1} (STP) using a mass flow controller
130 (Bronkhorst Hi-Tec, The Netherlands).

131 The DM contactor was operated both in lumen side mode (LS), where experiments
132 were carried out with the liquid flowing in the lumen side and vacuum pressure or
133 sweep gas applied in the shell side, and in shell side mode (SS) where the fluids were
134 swapped.

135 The selection between vacuum or sweep gas mode operations depends basically on
136 the aim of the process. Vacuum operation is the most feasible solution when the
137 recovery of degassing components is desired, since sweep gas operation would
138 involve subsequent costly separation/purification operations. If the process is carried
139 out only for liquid degassing, sweep gas mode can be selected since it usually needs
140 low energy consumption [20]. A combination mode (modest sweep with moderate
141 vacuum) could be used to enhance the degassing performance by increasing the gas

142 transfer driving force [21], but this intermediate situation induces an increase in
143 energetic costs [20].
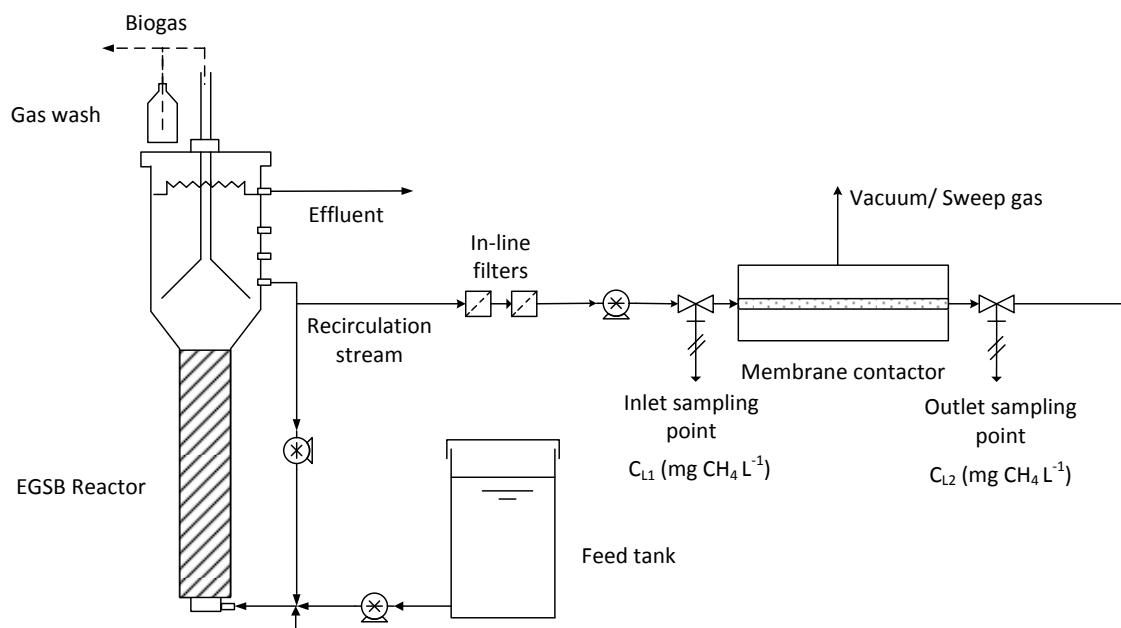
145 **Fig. 1**. Scheme of the set-up of the EGSB reactor and degassing membrane module

147 Cleaning of the DM module with deionised water at countercurrent flow during 30
148 minutes was done every day after experiments. A control experiment was repeated
149 every month to ensure that the DM module was operating without fouling and the
150 performance was not altered. Every short-term experiment was performed until stable
151 dissolved methane concentration in the outlet of the DM module was observed, usually
152 after 60-90 minutes of operation [17]. Discussion of results has been based on the
153 values obtained at this pseudo steady-state.

154 Finally, long-term experiments (> 30 hours without cleaning) were carried out to study
155 the effect of operation time on contactor fouling and performance, and to determine the
156 cleaning strategy for the application. Sweep gas mode configuration was selected for
157 these experiments for safety and practical aspects, since long-term operation with the
158 vacuum pump caused problems of stability and malfunction, as well as noise and
159 odours in the laboratory.

160 Two different cleaning protocols were used: conventional soft cleaning where only
161 deionised water was flowed in countercurrent for 30 min, and a chemical cleaning,
162 suggested by the DM supplier [21]: sequentially flowed in countercurrent 5% wt/wt of
163 sodium hydroxide aqueous solution (30 min), deionised water (5 min), 5% wt/wt of citric
164 acid aqueous solution (30 min) and deionised water (5 min).

166 2.2 *Determination of concentration of dissolved gases*

167 The headspace method was used in the analysis of D-CH$_4$. Liquid samples of 50 mL
168 were collected at the inlet and the outlet of the DM module and were injected in sealed

169　vials of 125 mL prefilled with helium. Vials were shaken vigorously for 30 seconds and
170　left at 25 ºC for 3 hours in an orbital shaker, to allow the gases to equilibrate. After
171　equilibration, 0.5 mL of the headspace gas was injected into a gas chromatograph
172　(Agilent GC 7820A, Spain), equipped with Agilent HP-PLOT/Q and Agilent HP-
173　MOLESIEVE columns. The D-CH_4 in liquid phase was calculated as:

$$C_L = \frac{C_{GH}\,(V_{GH} + H\,V_L)}{V_L} \tag{1}$$

174　where C_L is the concentration of dissolved methane in liquid phase (mg L^{-1}), C_{GH} the
175　methane gas concentration in headspace after equilibration (mg L^{-1}), V_L and V_{GH} are
176　volumes of liquid and gas space in the vial respectively (mL), and H the dimensionless
177　Henry's law constant for methane (29.55) at 25 ºC [22]. The performance of the
178　degassing module was evaluated with the removal efficiency (RE, %) of the
179　membrane, defined as:

$$RE = \frac{C_{L1} - C_{L2}}{C_{L1}} \cdot 100 \tag{2}$$

180　where C_{L1} and C_{L2} are the concentrations of dissolved methane in liquid phase (mg L^{-1})
181　at the inlet and outlet of the DM module, respectively. Samples from the inlet and outlet
182　were taken in duplicate and were analyzed in triplicate.

183

184　2.3 *Mass transfer evaluation*

185　Analysis of mass transfer is important both to assess the performance of the DM
186　contactor and to design/scale up a 'real' membrane unit. In our system, the
187　experimental overall mass transfer coefficient (K_{Lexp}, m s^{-1}) of CH_4 can be determined
188　from the mass balance applied at the liquid phase in the contactor by the following
189　differential expression:

$$Q_L \frac{dC}{dA} = -K_{Lexp}\,(C_L - C_L^*) \tag{3}$$

190　where Q_L is the liquid flow rate ($m^3\ s^{-1}$), A is the interfacial area (m^2), C_L is the
191　concentration of D-CH_4 in the liquid phase (mg L^{-1}) and C_L^* is the concentration in liquid
192　phase (mg L^{-1}) in equilibrium with the gas phase, which can be calculated from:

$$C_L^* = H \cdot C_G \tag{4}$$

193　where C_G is the concentration of CH_4 in the gas phase (mg L^{-1}). Integrating expression
194　(3) through the DM contactor yields:

$$\frac{K_{Lexp} A}{Q_L} = - \ln \left(\frac{C_{L2} - C_L^*}{C_{L1} - C_L^*} \right) \qquad (5)$$

195

196 The mass transfer process in the membrane contactor can be more easily visualized
197 and interpreted using the film theory approach. The overall mass transfer process
198 consists of three resistances in series: the liquid phase boundary layer (R_L), the
199 membrane (R_m), and the gaseous phase boundary layer (R_G). The overall mass
200 transfer coefficient (K_L) can be obtained by summing the partial resistances in series.
201 So, in a cylindrical geometry like in the hollow fibre contactor, the overall resistance
202 R_{total} (= 1/overall mass transfer) can be described by means of the equation:

$$R_{total} = \frac{1}{K_L A_L} = \frac{1}{Hk_G A_G} + \frac{1}{Hk_m A_{ml}} + \frac{1}{k_L A_L} = R_G + R_m + R_L \qquad (6)$$

203

204 where k_G, k_m and k_L stand for the mass transfer coefficients in the gas, membrane and
205 liquid, respectively, A_G and A_L are the membrane surfaces in contact with gas and
206 liquid respectively, A_{ml} is the logarithmic mean membrane surface, and H is the
207 equilibrium partition coefficient of the solute gas in between the gas and liquid phases
208 (Henry coefficient). Resistance into the gas phase can usually be assumed as
209 negligible, $R_G <<< R_m + R_L$, so in this case Eq. (6) can be reduced to:

$$R_{total} = \frac{1}{K_{Lexp} A_L} = \frac{1}{Hk_m A_{ml}} + \frac{1}{k_L A_L} = R_m + R_L \qquad (7)$$

210

211 ## 3. RESULTS AND DISCUSSION
212

213 *3.1 Characterization of the EGSB anaerobic effluent*

214 The EGSB reactor achieved a removal rate of around 31.4 kg COD m^{-3} d^{-1} resulting in
215 an organic removal efficiency > 95%. The biogas composition was 77% (v/v) CH_4 and
216 23% (v/v) CO_2 and the methane flow rate was 1.65 L h^{-1} (STP). The average dissolved
217 methane (D-CH_4) measured in the water effluent of the reactor was usually around 30 ±
218 5 mg L^{-1}. This indicates an oversaturation of the anaerobic effluent by a factor of 2 with
219 respect to the equilibrium D-CH_4 concentration of 15 mg L^{-1} at experimental conditions
220 [22]. D-CH_4 oversaturation is commonly observed in anaerobic reactors with
221 oversaturation factors ranging from 1.3 to 6.9 [5–7,12,23]. Solids concentrations were
222 measured before and after the filter sited previous membrane module. No appreciable
223 differences were observed, indicating that water quality was not altered. Values of total
224 and volatile solids were 3850 ±75 and 250 ±25 mg L^{-1}, respectively.

225 At these operational conditions, the amount of methane lost in aqueous effluent
226 represents around 1% of the total methane produced in the EGSB anaerobic reactor.
227 Quite disparate values of percentage of methane lost in anaerobic effluents can be
228 found in the literature [1,3,4,16]. This disparity of percentage of methane lost can be
229 explained taking into account that the amount of methane (L h^{-1}) lost in aqueous
230 effluent depends on water flow and temperature, which affect to equilibrium
231 concentration of solved methane, but it is almost independent on organic load and
232 reactor efficiency. So, high values of percentage of methane lost should be obtained for
233 low strength wastewater treatments and low values for high strength wastewater
234 treatments. Luo et al. [16] obtained similar values to those reported in this study,
235 ranging from 1.6 to 5.6%, using a degassing membrane coupled to an upflow
236 anaerobic sludge blanket (UASB) reactor, using similar organic load (20 kg COD m^{-3} d^{-1}
237), and higher percentages (> 11%) have frequently been reported [1,3,4] for different
238 low strength wastewater treatments (1.1-0.2 kg COD m^{-3} d^{-1}). In any case, the feasibility
239 of the membrane process will depend on ability of the contactor module to recover the
240 amount of methane (L h^{-1}) lost in aqueous effluent but not on methane production of
241 anaerobic reactor.

242

243 *3.2 Degassing membrane performance*

244 Regarding the removal of D-CH$_4$ in the DM module, Fig. 2 shows the effect of the liquid
245 flow rate on the removal efficiency. Some of the results presented have been
246 previously reported in a former work [17] where a comparison of membrane modules
247 (porous and non-porous) was carried out, but the conjunction of the results in this study
248 (reported and not previously reported) provides a more deep knowledge of the
249 operation conditions. For sake of clarity previous reported experiments have been
250 plotted in grey filled symbols in Fig. 2 and 3. As can be observed in Fig. 2a,
251 independently of the vacuum/permeate pressure or of the mode of operation (LS or
252 SS), methane recovery decreases with increasing liquid flow rate. A similar trend has
253 previously been reported for membrane degassing of methane [15] or similar
254 applications [9,24].

255 The maximum removal efficiencies obtained in our experiments at vacuum operation
256 mode were of around 77% for experiments at the highest vacuum (800 mbar) and the
257 lowest liquid flow rate (~0.4 L h^{-1}), and operated with the liquid in the lumen side.
258 Regarding the influence of the transmembrane pressure on the recovery/removal
259 efficiency of dissolved gases, it has been reported [9,25] that it would depend on both
260 the nature of the degassed compound and the rest of the operational conditions, such
261 as the liquid flow rate or sweep gas introduction. The positive influence of the vacuum
262 pressure on the removal efficiency could also denote that membrane resistance had a
263 considerable role in the overall resistance of the process [17,26], as will be discussed
264 later.

265 According to the DM supplier, the most efficient mode of operation of this type of
266 module for air liquid degassing is with the liquid on the shell side (outside the hollow
267 fibres) [21]. However, this mode of operation typically has a lower trans-membrane
268 pressure (TMP) limitation compared to operating with the liquid on the lumen side

269　(Table 1). The reason for the lower pressure limit from shell to lumen is because the
270　hollow fibres may collapse and be damaged if the pressure from the outside of the
271　hollow fibre to the lumen side of the hollow fibre exceeds 1050 mbar. On the other
272　hand, if the pressure from the lumen side to the outside of the hollow fibre exceeds
273　3100 mbar, the hollow fibres may over-distend and potentially be damaged [21].
274　Nevertheless, it has been frequently reported that the best performance of different
275　modules for liquid degassing is achieved when the liquid flows on the lumen side
276　[24,27]. The best or worst performance of the operation mode can usually be related to
277　the flow settings (e.g. Reynolds number or dead zones), which condition the mass
278　transfer resistance.
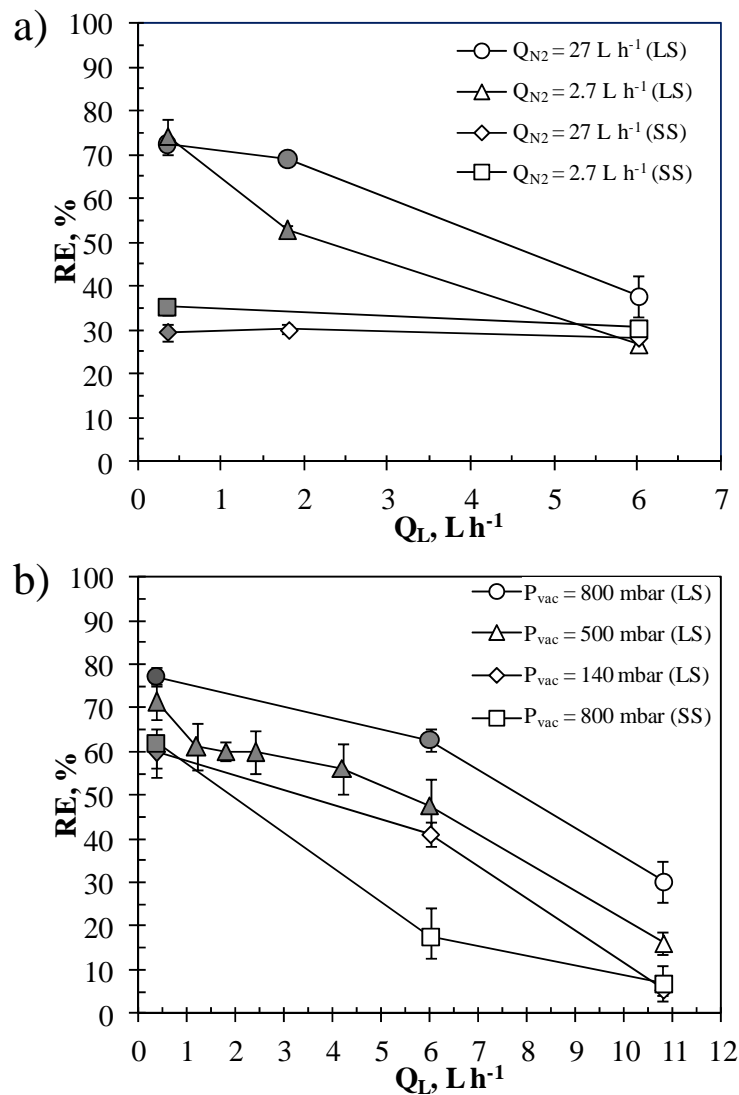
279

280　Fig. 2. Effect of liquid flow rate on the removal efficiency of D-CH_4 for a) vacuum
281　experiments and b) sweep gas experiments. LS: Liquid in lumen side. SS: Liquid in
282　shell side. Filled grey symbols data from [17].

283

284　In our experiments, the membrane performance in shell and lumen side modes was
285　also compared at the highest vacuum pressure (800 mbar, Fig. 2a). As can be seen,

9

286 and in contrast to what was indicated by the DM supplier [21], the shell side mode
287 showed usually 20-25% lower removal efficiency than the lumen side mode at the
288 same operational conditions, which could be attributed to a higher cross-section in the
289 shell part of the module, which means a lower liquid velocity and a higher probability of
290 channelling.

291 Thus it is important to know the influence of the fluid operational conditions on each
292 hollow fibre membrane before selecting the mode of operation and, depending on the
293 operating conditions of the system, the maximum allowable trans-membrane pressure
294 (TMP) may limit the way a module should be used [21].

295 The results of experiments operating with N_2 as sweep gas can be seen in Fig. 2b
296 under configurations of lumen and shell side modes. For lumen side operation (LS) the
297 trends were similar to that described at vacuum operation: RE decreased with the liquid
298 flow rate, and increased with the sweep gas flow rate (15–20% of difference at Q_{N2} of
299 2.7 and 27.0 L h^{-1}), except for the experiments at the minimum liquid flow rate 0.4 L h^{-1},
300 where the results were practically the same at both Q_{N2} tested. By contrast,
301 experiments carried out in shell side mode (SS) showed a different behaviour. In this
302 mode of operation no significant influence of gas or liquid flow rate on methane RE was
303 observed, with values of RE around 30–35% at all the flows tested. This 'plateau'
304 performance may indicate that when the module is operated in shell side mode,
305 transport through the PDMS membrane is the predominant resistance to overall mass
306 transfer. Besides, the fact that the RE of the experiments in LS with higher liquid flow
307 rates and gas is substantially the same as that obtained with the SS experiments could
308 corroborate this hypothesis, since in these conditions less resistance to mass transfer
309 would exist in the liquid phase and gas.

310 When the performance of vacuum and sweep gas type operation is compared (Figs. 2
311 and 3), different influences of the liquid flow rate were observed. For the lowest liquid
312 flow rate tested (0.5 L h^{-1}), vacuum operation performs better only for experiments
313 carried out at the maximum vacuum operation (800 mbar), but a sharper decline in RE
314 with the liquid flow rate was observed for sweep gas operation, and at medium and
315 high liquid flow, even operating at the minimum vacuum tested (140 mbar), the vacuum
316 operation experiments show better RE than the sweep gas experiments.

317

318 *3.3 Mass transfer study*

319 As has been introduced previously, the overall mass transfer coefficient K_{Lexp} can be
320 obtained experimentally from the unit membrane degassing mass balance at the liquid
321 phase (Eq. (5)). Variation with the liquid flow rate at different operation modes and
322 vacuum pressures can be found in Fig. 3a.

323 According to Eqs. (6) and (7), if the resistance of the liquid phase is not negligible, an
324 increase in liquid flow rate must promote higher values of the overall coefficient. As can
325 be seen in Fig. 3a, a positive dependence was obtained for liquid flow rate below 6 L h^{-}
326 ^{1}, especially in LS mode operation, indicating that the liquid mass transfer resistance
327 can have a predominant role. Nevertheless, when the flow rate was increased until

328 near the liquid flow rate limit of the unit (12.0 L h^{-1}, Table 1), the mass transfer
329 coefficient drastically decreased.

330 This unusual behaviour, the decrease of the mass transfer coefficient with the liquid
331 flow rate, could denote that the membrane unit has an operational flow rate limit from
332 which the fibres may suffer overpressure that can deform or compress them, which
333 would reduce its permeability, and increase the membrane resistance.

334
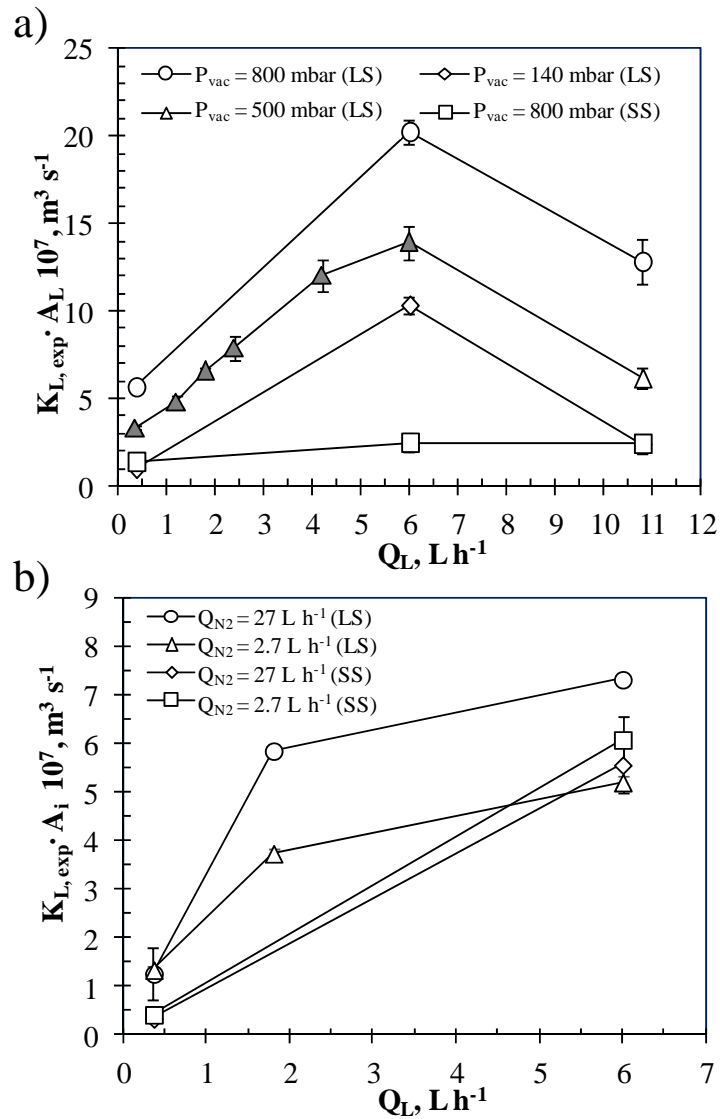
335

336 Fig. 3. Experimental mass transfer coefficient ($K_{Lexp} \cdot A_L$) for a) vacuum experiments
337 and b) sweep gas experiments. LS: Liquid in lumen side. SS: Liquid in shell side. Filled
338 grey symbols data from [17]

339

340 As has usually been reported for similar operations [6], the methane mass transfer was
341 improved by increasing the transmembrane pressure, and the experiment carried out at
342 800 mbar of vacuum pressure showed the highest overall mass transfer coefficients

343 (Fig. 3a). These results could suggest that the membrane resistance was non-
344 negligible at the operational conditions studied and, as has been previously reported
345 [26,28], the membrane mass transfer coefficient (k_m) can be positively influenced by
346 the vacuum pressure of the permeate. In this sense, the membrane resistance
347 coefficient for dense membranes has been related to the membrane thickness, partial
348 pressure of the permeate compound, and permeability coefficient [29], which depends
349 on the properties of both the membrane and compound (barrer = 7.5005 x 10^{-18} m^2s^-
350 $^1Pa^{-1}$ – STP). For PDMS membranes, values of the methane permeability coefficient at
351 ambient conditions are usually reported from 850 to 1600 barrer [30–32], with a value
352 of 950 barrer [33] suggested by the module supplier.

353

354 As expected from the removal efficiency results, comparison of the shell and lumen
355 side operations mode (800 mbar) showed lower overall mass transfer coefficients for
356 the shell side at vacuum experiments, probably due to their lower liquid velocity.

357 The values of the mass transfer coefficient for sweep gas experiments can be found in
358 Fig. 3b. K_L increased with the liquid and gas flow rate, except for the shell side mode
359 (gas into the fibres), where the influence of the gas flow rate on the K_L was minimal.
360 The fact that at the highest liquid flow rate the overall mass transfer coefficients are
361 quite similar, independently of the operation mode, seems to confirm the importance of
362 membrane resistance at these operational conditions also in the sweep gas
363 experiments. Assuming that the membrane mass resistance was predominant at the
364 highest flow rate in the shell side mode (Fig. 3b), the membrane mass transfer
365 coefficient, $k_{m,}$, can be obtained from Eq. (7) with a value near the range (10^{-5}- 10^{-6} m s$^-$
366 ^{1}) of that reported for dense materials of polymer with the same thickness and
367 permeability characteristics [18,29].

368 In Fig. 4a modified Wilson plot is presented, where the different transport resistances
369 (R_j = 1 / k_jA_j) for experiments at 500 mbar vacuum are shown. As assumed, the gas
370 phase resistance can be considered as negligible (<0.5% of overall resistance),
371 independent of the estimation equation [34,35], and it has not been taken into
372 consideration for simplification purposes. The white point corresponds to the highest
373 tested liquid flow rate (Q_L = 11 L h^{-1}), where, as discussed previously, an unusual
374 behaviour was observed. This point has not been considered for correlations or further
375 discussion. The solid line stands for the theoretical liquid resistance (R_L= 1/k_LA_i) where
376 the liquid mass transfer coefficient, k_L, has been estimated from the Leveque equation
377 [36]:

$$\frac{k_L d_i}{D} = 1.62 \left[\frac{d_i^2 v_L}{LD}\right]^{0.333} \tag{8}$$

378 where d_i (m) is the fibre inner diameter, L(m) the length, v_L (m s^{-1}) the liquid velocity,
379 and D the molecular diffusivity of methane in water, reported as 1.76 10^{-9} m^2 s^{-1} [37].
380 This equation has been demonstrated extensively as correlating the mass transfer in
381 the lumen side under laminar flow [10,11].

382   As we can see in Fig. 4, the experimental overall resistance was significantly lower
383   than the estimation of the liquid phase resistance, indicating that the mass transfer
384   resistance in the liquid phase is much lower than that predicted by the theoretical
385   correlations. This enhancement of component mass transfer has been described
386   previously when oversaturation conditions of degassed component exist in the liquid
387   phase [15] and it should be taken into account in design considerations, to avoid
388   excessive oversizing of units. In this sense, to include in the mass transfer resistance
389   model the effect of methane oversaturation, this study proposes the introduction of an
390   enhancement factor for driving the mass transfer (E) in liquid phase transfer associated
391   with oversaturation, analogous to that used when chemical reactions take place in the
392   liquid phase. So, the mass transfer resistance Eq. (7) can be expressed as:

$$\frac{1}{K_{Lexp}A_L} = \frac{1}{Hk_mA_{ml}} + \frac{1}{E\,k_LA_i} \tag{9}$$

393

394   The dotted line in Fig. 4 represents the linear correlation of the experimental overall
395   resistance (black square points) with Eq. (9) considering the Leveque equation for k_L.
396   As can be seen, a relatively good correlation (r^2 = 0.9) with a value for the
397   enhancement factor (E) of 1.6 from the slope of the linear correlation was obtained.
398   The dashed line shows the membrane resistance obtained from the intercept (R_m =
399    $1/Hk_mA_{ml}$ = 1.64 10^5 s m^{-3}) of the linear correlation. This value is quite similar to that
400   reported previously [18,29] for this compound, and material permeability and thickness.
401   As can be seen (Fig. 4), the membrane resistance seemed non-negligible, ranging
402   from 7 to 20% of overall resistance, especially for high liquid velocities.

403
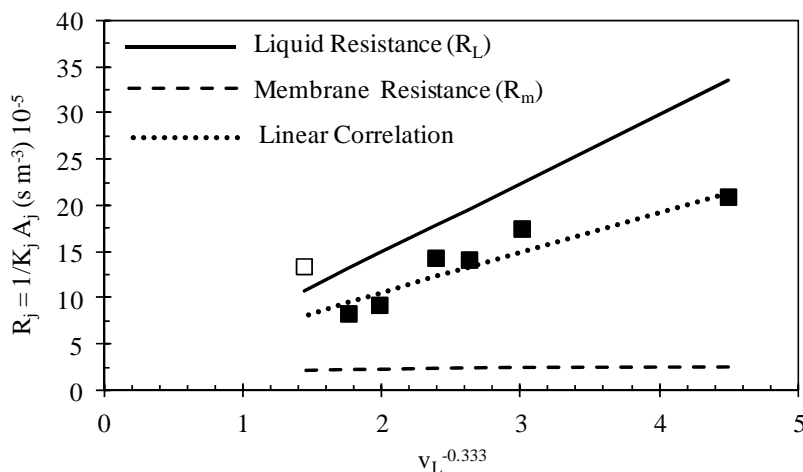
404

405   Fig. 4. Modified Wilson plot of results in lumen side mode at. 500 mbar of vacuum
406   pressure. Points: experimental overall resistance (R_{total}= $1/K_{Lexp}A_i$). Solid line: liquid
407   resistance (R_L= $1/k_LA_i$) estimated from Leveque equation [36]. Dotted line: linear
408   correlation of experimental points with Eq. (9). Dashed line: membrane resistance (R_m).

409

410

3.4 Long-term performance: fouling

The period from which membrane fouling considerably affects the DM performance and when it must be cleaned is especially important in real industrial continuous treatments, where cleaning stages must be planned and taken into account for economic considerations. The appearance of the fouling phenomenon in DMs for methane recovery in effluents of anaerobic treatments has not been studied in the specific literature and most previous studies [4,15,17] have been carried out at a relatively short time-on-stream (<1 hour), without fouling interference. Only the studies developed by Bandara et al. [12,13] indicated that membrane fouling of the DM was insignificant for their long-term experiments (>30 days).

As explained earlier, long-term experiments were performed in order to determine both the possible influence of fouling on the contactor performance and the frequency of cleaning that should be used to maintain the desired methane recovery/removal capability. These experiments were carried out in the sweep gas mode configuration. Initially, a lumen side mode experiment was carried out, as shown in Fig. 5a. As can be seen in this figure, the performance in this experiment was kept almost stable/constant (RE around 60–65%) for approximately 120 hours of operation, but after this period an appreciable and continuous decrease in efficiency was observed. This decrease was attributed to fouling phenomena on the membrane, which was corroborated, since, after conventional cleaning with deionised water, the initial activity was completely recovered (around 65% of RE). Despite the use of a filter that prevented the passage of particles > 40 microns, the appearance of fouling was relatively early, but seemed reversible with a soft cleaning. Natural organic matter related to microbial and extracellular polymer substances has been described as the major type of foulant in biological wastewater treatment units [38] and most of them can present a size lower than 40 microns. Biofouling has been described as a major concern in anaerobic membrane bioreactors, limiting more widespread application of this system in wastewater treatments [39].

As can be seen in Fig. 5b, the results for shell side mode operation at the same liquid operational conditions were quite different. The duration of the initial period of stable performance (RE around 35%) was considerably lower than that observed in lumen operation (< 50 hours). This faster deactivation may be related to the lower velocity of the liquid in the SS operation, which may favour the deposition of particles from the biological process and therefore the fouling effect. Moreover, with conventional cleaning (water cleaning 1 in Fig. 5), RE recovered only partially (around 20%) but did not reach the initial performance and after a period of almost 50 hours the performance decreased again. As the RE did not completely recover, it was assumed that a residual fouling, that was difficult to remove with water, increased the resistance to methane mass transfer, so a chemical cleaning protocol was used to try to remove this fouling and restore the initial performance. Two consecutive chemical cleanings (chemical cleanings 1 and 2 in Fig. 5b) were needed to restore the RE to values similar to the initial ones, but a decrease of performance appeared only 20 hours later. Further water or chemical cleaning protocols did not restore the initial performance and a performance decrease appeared almost immediately (1–2 hours). This behaviour could

14

be attributed to an irreversible/recalcitrant biofouling promoted by the growth of biologically active microorganisms to form biofilms. A less probable damage to the membrane from the use of the chemical cleaning protocol could also provoke the same effect. In any case, this DM unit was discarded for the rest of the experiments.
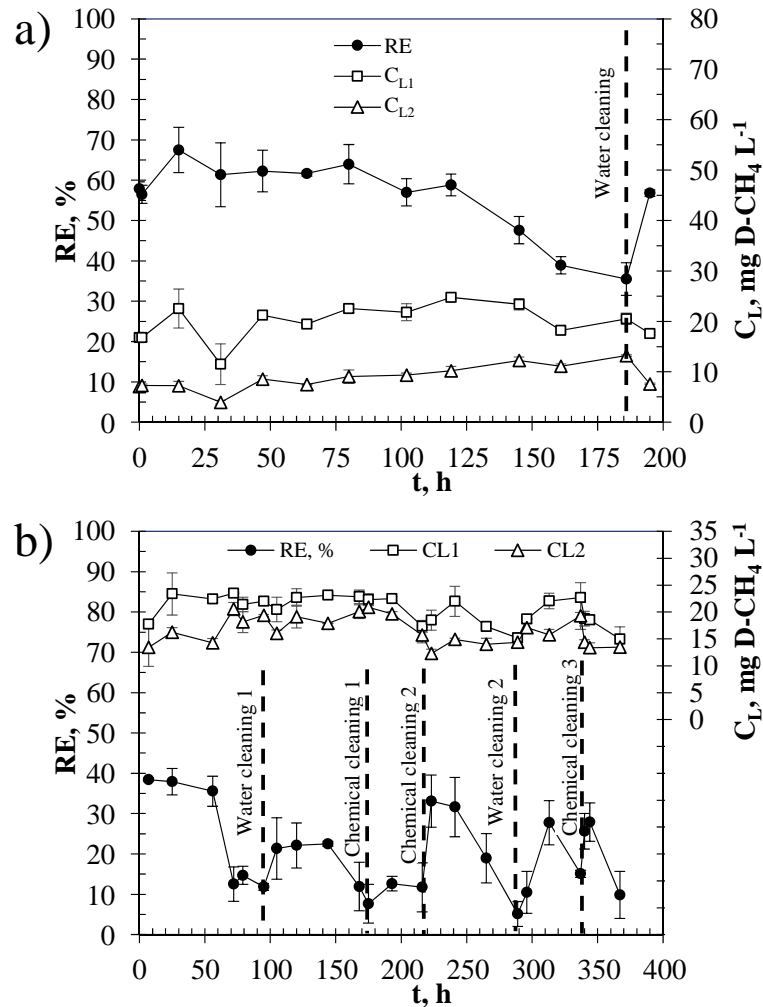
Fig. 5. Effect of long-term operation on RE. a) Lumen side mode: Q_L=1.8 L h^{-1}. Q_{N2}= 12 L h^{-1}. b) Shell side mode: Q_L=1.8 L h^{-1}. Q_{N2}= 2.7 L h^{-1}.

These results highlight the importance of choosing an appropriate strategy for membrane fouling control and membrane cleaning [40], especially in biological treatments where, additionally, a complex chemistry is involved and different mechanisms and synergistic effects can promote the appearance of fouling [38]. So, taking into account that during the short-term experiment phase, the occurrence of fouling was not observed, despite the more than 5000 hours of accumulated operation (3000 h in LS and 2250 h in SS), a similar cleaning strategy to that used in that phase, based on a daily water backwashing of about 30 minutes, could be proposed for this process.

473

474   *3.5 Feasibility: energy and economic considerations*

475   As was argued formerly, vacuum operation offers the potential to deliver much higher
476   recovered gas purities, since it minimises gas-side dilution by avoiding the addition of
477   dilutive sweep gas, and an elevated concentration of methane can be obtained [20].
478   Therefore, only this operation mode has been evaluated for the energy and cost
479   efficiency.

480   In order to determine the efficiency of the recovery of methane, a comparison between
481   energy recovered as methane and the energy demand of the operation must be carried
482   out. In this case, the power demand of vacuum (blower) and liquid flow (pump)
483   operations will be considered. Blower/compressor power consumption (W) can be
484   calculated for an isentropic process from the following expression [4]:

$$W(J\ kg^{-1})= \frac{\gamma}{\gamma - 1}\frac{R\ T_a}{M}\left[\left(\frac{P_D}{P_A}\right)^{\frac{\gamma-1}{\gamma}} - 1\right]$$ (10)

485   P_D and P_A are discharge and suction pressure, respectively, γ is the isentropic
486   expansion coefficient of gas, R is the constant of ideal gases, M is the molecular weight
487   of the gas, and T_a is the temperature of the suction. Assuming a vacuum pump
488   efficiency of 0.65, the power demand can be calculated. For liquid flow, the power
489   consumption in the membrane can be estimated from:

$$W(J\ kg^{-1})= \frac{P_I - P_O}{\rho} + \sum F$$ (11)

490   where P_I and P_O are the inlet and outlet pressure, $\sum F$ is the friction loss (estimated as
491   20% of the total power demand) and ρ is the liquid density. A pump efficiency of 0.65
492   was also assumed in this study.

493   Assuming an electrical conversion efficiency of methane of 35%, the energy required in
494   vacuum operation ranged from 0.2% to 3% of the recovered energy as methane in the
495   membrane for 140 mbar and 800 mbar of vacuum pressures, respectively. The pump
496   operation was always lower than 0.01% of the recovered energy and therefore it can
497   be considered as negligible. As the amount of methane recovered increased with
498   vacuum pressure and RE, to compare different operational conditions the parameter
499   Saved Energy has been defined as the difference between the recovered electrical
500   energy and demand of vacuum operation energy per cubic meter of treated effluent.

501   Fig. 6 shows the variation of the recovered energy per cubic meter of effluent versus
502   the anaerobic effluent flow rate. As observed, the saved energy was positive in all
503   cases, and showed an optimum value for liquid flow rate of around 2–6 L h^{-1} for lumen
504   side operation. These results show that, even when using conservative values for the
505   process included in the energy balance, a net energy production can be obtained from
506   the recovery of methane in anaerobic effluents. Similar conclusions have been recently
507   reported [4,15].

508   In addition, the renewable energy that can be produced from the recovered methane
509   can offset the carbon footprint of D-CH_4 in anaerobic effluents, which indicates that
510   integrating this technology in the anaerobic treatment of wastewater can even become
511   carbon-positive. The environmental interest of this technology is clearly demonstrated
512   when the emission to the atmosphere of around 0.20 kg CO_2 equivalent m^{-3} effluent is
513   avoided with every 25% of removal/recovery efficiency (RE) of the process. In an
514   anaerobic treatment of 100 m^3 effluent h^{-1} and for a RE of 60–70%, it would be possible
515   to avoid the emission of 400–500 tons of CO_2 equivalent per year.
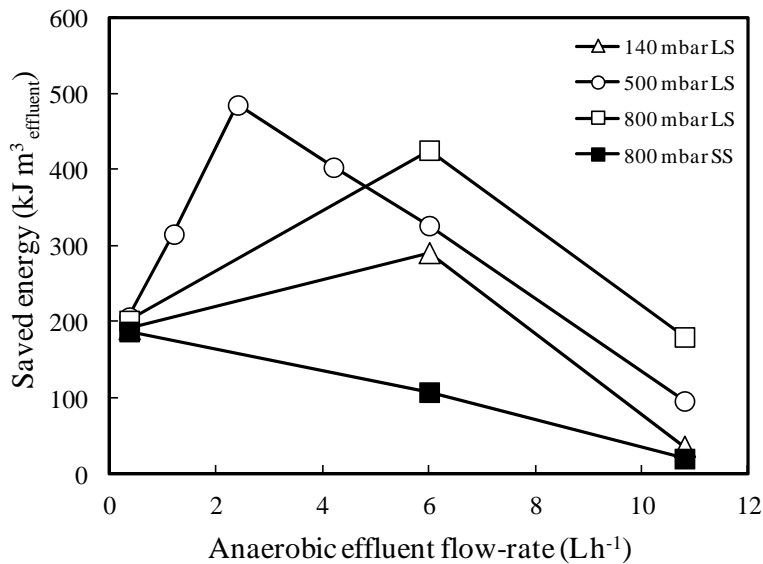
516

517   Fig. 6. Saved energy at different operational conditions. LS: lumen side, SS: shell side.

518

519   From an economic point of view, the energy saved seems relatively low: for example,
520   500 kJ m^{-3} effluent (near the maximum value in Fig. 6) means that approximately 0.140
521   kWh m^{-3} effluent can be saved. These values are in agreement with those recently
522   reported [4,6,15]. Assuming an electricity cost of 0.100 € kWh^{-1}, around 0.014 € per
523   cubic meter of treated effluent could be obtained in the methane recovery operation. In
524   these conditions, for an anaerobic treatment of 100 m^3 effluent h^{-1}, the economic saving
525   from the produced electricity would be of only around 10 000–12 500 € per year.
526   Taking into account that capital cost of membrane process was reported to be in the
527   range of 1 000-1 200 € per m^3 h^{-1} [41], that annual saving could serve to fund at least
528   partially investment and/or operational costs (personnel, cleaning and others), but does
529   not seem sufficient to fully assure the financial viability of the process. Further
530   reduction in capital cost of membranes seems still necessary to guarantee the
531   economic yield of the process.

532

533   **4. Conclusions**

534   The performance and viability of the use of a polydimethylsiloxane hollow fibre
535   membrane module for in situ methane recovery/removal from the effluent of an

536 Expanded Granular Sludge Bed (EGSB) anaerobic reactor has been studied. The
537 methane concentration in the biological reactor effluent was around two times higher
538 than saturation equilibrium. The maximum removal efficiencies obtained in our
539 experiments at vacuum operation mode were of around 77% for experiments at the
540 highest vacuum (800 mbar) and the lowest liquid flow rate ($\sim$0.4 L h^{-1}), when operated
541 with the liquid in the lumen side. Independent of the operational conditions, shell side
542 mode showed lower removal efficiency than lumen side mode, which was attributed to
543 the lower liquid velocity and a higher probability of channelling of the shell part of the
544 module. The comparative performance of vacuum and sweep gas type operations
545 depended on the liquid flow rate and vacuum pressure.

546 Mass transport analysis denoted that the methane transfer was enhanced by liquid
547 oversaturation and the overall mass transfer coefficients were considerably higher than
548 predicted by theoretical models. An enhancement factor for liquid phase has been
549 proposed to correlate the experimental results, with a value of 1.6 for 500 mbar
550 vacuum pressure operation in LS mode. Additionally, the membrane resistance
551 seemed non-negligible, ranging from 10 to 30% of overall resistance, especially for low
552 liquid velocities.

553 In the first attempt in the literature to study the long-term behaviour of a DM module for
554 methane degassing, a faster deactivation in the SS mode operation was observed,
555 related to the lower velocity of the liquid in this mode that can favour the fouling effect.
556 Fouling seemed to depend little on the mode and operational conditions, and a
557 relatively frequent cleaning with water might be carried out to ensure preservation of
558 the membrane efficiency during long periods.

559 The energy balance analysis showed that energy production exceeded the system
560 energy requirements for all the operation conditions, although it does not seem enough
561 to guarantee the economic yield of the process. A considerable reduction of CO_2
562 equivalent emissions showed the positive environmental impact of this technology.

563

Acknowledgements

569

References

571 [1]   F.Y. Cakir, M.K. Stenstrom, Greenhouse gas production: a comparison between
572   aerobic and anaerobic wastewater treatment technology., Water Res. 39 (2005)
573   4197–203. doi:10.1016/j.watres.2005.07.042.

574 [2]   A.L. Smith, L.B. Stadler, N.G. Love, S.J. Skerlos, L. Raskin, Perspectives on
575   anaerobic membrane bioreactor treatment of domestic wastewater: a critical
576   review., Bioresour. Technol. 122 (2012) 149–59.
577   doi:10.1016/j.biortech.2012.04.055.

578 [3] Z. Alshboul, J. Encinas-Fernández, H. Hofmann, A. Lorke, Export of dissolved
579 methane and carbon dioxide with effluents from municipal wastewater treatment
580 plants, Environ. Sci. Technol. 0 (2016). doi:10.1021/acs.est.5b04923.

581 [4] B.C. Crone, J.L. Garland, G.A. Sorial, L.M. Vane, Significance of dissolved
582 methane in effluents of anaerobically treated low strength wastewater and
583 potential for recovery as an energy product: A review, Water Res. 104 (2016)
584 520–531. doi:10.1016/j.watres.2016.08.019.

585 [5] C.L. Souza, C.A.L. Chernicharo, S.F. Aquino, Quantification of dissolved
586 methane in UASB reactors treating domestic wastewater under different
587 operating conditions, Water Sci. Technol. 64 (2011) 2259–2264.
588 doi:10.2166/wst.2011.695.

589 [6] J. Cookney, E. Cartmell, B. Jefferson, E.J. McAdam, Recovery of methane from
590 anaerobic process effluent using poly-di-methyl-siloxane membrane contactors.,
591 Water Sci. Technol. 65 (2012) 604–10. doi:10.2166/wst.2012.897.

592 [7] H. Yeo, J. An, R. Reid, B.E. Rittmann, H.S. Lee, Contribution of Liquid/Gas
593 Mass-Transfer Limitations to Dissolved Methane Oversaturation in Anaerobic
594 Treatment of Dilute Wastewater, Environ. Sci. Technol. 49 (2015) 10366–10372.
595 doi:10.1021/acs.est.5b02560.

596 [8] M. Bani Shahabadi, L. Yerushalmi, F. Haghighat, Impact of process design on
597 greenhouse gas (GHG) generation by wastewater treatment plants, Water Res.
598 43 (2009) 2679–2687. doi:10.1016/j.watres.2009.02.040.

599 [9] A. Sengupta, P.A. Peterson, B.D. Miller, J. Schneider, C.W. Fulk, Large-scale
600 application of membrane contactors for gas transfer from or to ultrapure water,
601 Sep. Purif. Technol. 14 (1998) 189–200. doi:10.1016/S1383-5866(98)00074-4.

602 [10] M. Stanojević, B. Lazarević, D. Radić, Review of membrane contactors designs
603 and applications of different modules in industry, FME Trans. 31 (2003) 91–98.

604 [11] A. Gabelman, S.-T. Hwang, Hollow fiber membrane contactors, J. Memb. Sci.
605 159 (1999) 61–106. doi:10.1016/S0376-7388(99)00040-X.

606 [12] W.M.K.R.T.W. Bandara, H. Satoh, M. Sasakawa, Y. Nakahara, M. Takahashi, S.
607 Okabe, Removal of residual dissolved methane gas in an upflow anaerobic
608 sludge blanket reactor treating low-strength wastewater at low temperature with
609 degassing membrane., Water Res. 45 (2011) 3533–40.
610 doi:10.1016/j.watres.2011.04.030.

611 [13] W.M.K.R.T.W. Bandara, T. Kindaichi, H. Satoh, M. Sasakawa, Y. Nakahara, M.
612 Takahashi, et al., Anaerobic treatment of municipal wastewater at ambient
613 temperature: Analysis of archaeal community structure and recovery of
614 dissolved methane., Water Res. 46 (2012) 5756–64.
615 doi:10.1016/j.watres.2012.07.061.

616 [14] W.M.K.R.T.W. Bandara, M. Ikeda, H. Satoh, M. Sasakawa, Y. Nakahara, M.
617 Takahashi, et al., Introduction of a Degassing Membrane Technology into
618 Anaerobic Wastewater Treatment, Water Environ. Res. 85 (2013) 387–390.
619 doi:10.2175/106143013X13596524516707.

620 [15] J. Cookney, A. Mcleod, V. Mathioudakis, P. Ncube, A. Soares, B. Jefferson, et
621 al., Dissolved methane recovery from anaerobic effluents using hollow fibre
622 membrane contactors, J. Memb. Sci. 502 (2016) 141–150.

623   doi:10.1016/j.memsci.2015.12.037 doi:10.1016/j.memsci.2015.12.037.

624   [16]   G. Luo, W. Wang, I. Angelidaki, A new degassing membrane coupled upflow
625   anaerobic sludge blanket (UASB) reactor to achieve in-situ biogas upgrading
626   and recovery of dissolved CH4 from the anaerobic effluent, Appl. Energy. 132
627   (2014) 536–542. doi:10.1016/j.apenergy.2014.07.059.

628   [17]   M. Henares, M. Izquierdo, J.M. Penya-Roja, V. Martínez-Soria, Comparative
629   study of degassing membrane modules for the removal of methane from
630   Expanded Granular Sludge Bed anaerobic reactor effluent, Sep. Purif. Technol.
631   170 (2016) 22–29. doi:http://dx.doi.org/10.1016/j.seppur.2016.06.024.

632   [18]   E. Chabanon, B. Belaissaoui, E. Favre, Gas–liquid separation processes based
633   on physical solvents: opportunities for membranes, J. Memb. Sci. 459 (2014)
634   52–61. doi:10.1016/j.memsci.2014.02.010.

635   [19]   C. Lafita, J.M. Penya-roja, C. Gabaldón, Anaerobic removal of 1-methoxy-2-
636   propanol under ambient temperature in an EGSB reactor, Bioprocess Biosyst.
637   Eng. (2015) 2137–2146. doi:10.1007/s00449-015-1453-0.

638   [20]   C. Vallieres, E. Favre, Vacuum versus sweeping gas operation for binary
639   mixtures separation by dense membrane processes, J. Memb. Sci. 244 (2004)
640   17–23. doi:10.1016/j.memsci.2004.04.023.

641   [21]   PermSelect, Operating Guidelines for PermSelect® Modules Liquid Contacting,
642   (2016). http://permselect.com/files/PermSelect Operating Instructions - Liquid
643   Contacting.pdf (accessed April 1, 2017).

644   [22]   R. Sander, Compilation of Henry 's Law Constants for Inorganic and Organic
645   Species of Potential Importance in Environmental Chemistry, Database. 20
646   (1999) 107.

647   [23]   A.L. Smith, S.J. Skerlos, L. Raskin, Psychrophilic anaerobic membrane
648   bioreactor treatment of domestic wastewater, Water Res. 47 (2013) 1655–1665.
649   doi:10.1016/j.watres.2012.12.028.

650   [24]   Z.-G. Peng, S.-H. Lee, T. Zhou, J.-J. Shieh, T.-S. Chung, A study on pilot-scale
651   degassing by polypropylene (PP) hollow fiber membrane contactors,
652   Desalination. 234 (2008) 316–322. doi:10.1016/j.desal.2007.09.100.

653   [25]   C.I. McDermott, S.A. Tarafder, O. Kolditz, C. Schüth, Vacuum assisted removal
654   of volatile to semi volatile organic contaminants from water using hollow fiber
655   membrane contactors. II: A hybrid numerical-analytical modeling approach, J.
656   Memb. Sci. 292 (2007) 17–28. doi:10.1016/j.memsci.2007.01.009.

657   [26]   J. Li, L.-P. Zhu, Y.-Y. Xu, B.-K. Zhu, Oxygen transfer characteristics of
658   hydrophilic treated polypropylene hollow fiber membranes for bubbleless
659   aeration, J. Memb. Sci. 362 (2010) 47–57. doi:10.1016/j.memsci.2010.06.013.

660   [27]   X. Tan, G. Capar, K. Li, Analysis of dissolved oxygen removal in hollow fibre
661   membrane modules: effect of water vapour, J. Memb. Sci. 251 (2005) 111–119.
662   doi:10.1016/j.memsci.2004.11.005.

663   [28]   T. Ahmed, M.J. Semmens, M.A. Voss, Oxygen transfer characteristics of hollow-
664   fiber, composite membranes, Adv. Environ. Res. 8 (2004) 637–646.
665   doi:10.1016/S1093-0191(03)00036-4.

666   [29]   P.T. Nguyen, E. Lasseuguette, Y. Medina-Gonzalez, J.C. Remigy, D. Roizard, E.

667 Favre, A dense membrane contactor for intensified CO2 gas/liquid absorption in
668 post-combustion capture, J. Memb. Sci. 377 (2011) 261–272.
669 doi:10.1016/j.memsci.2011.05.003.

670 [30] S. Heile, S. Rosenberger, A. Parker, B. Jefferson, E.J. McAdam, Establishing
671 the suitability of symmetric ultrathin wall polydimethylsiloxane hollow-fibre
672 membrane contactors for enhanced CO_2 separation during biogas upgrading, J.
673 Memb. Sci. 452 (2014) 37–45. doi:10.1016/j.memsci.2013.10.007.

674 [31] D.C. Nymeijer, B. Folkers, I. Breebaart, M.H. V Mulder, M. Wessling, Selection
675 of Top Layer Materials for Gas-Liquid Membrane Contactors, J. Appl. Polym.
676 Sci. 92 (2004) 323–334. doi: 10.1002/app.20006.

677 [32] T.C. Merkel, V.I. Bondar, K. Nagai, B.D. Freeman, I. Pinnau, Gas sorption,
678 diffusion, and permeation in poly(dimethylsiloxane), J. Polym. Sci. Part B Polym.
679 Phys. 38 (2000) 415–434. doi:10.1002/(SICI)1099-
680 0488(20000201)38:3<415::AID-POLB8>3.0.CO;2-Z.

681 [33] J.P. Montoya, Membrane Gas Exchange: Using Hollow Fiber Membranes to
682 Separate Gases from Liquid and Gaseous Streams, MedArray, Inc. (2010).
683 https://permselect.com/files/Using_Membranes_for_Gas_Exchange.pdf
684 (accessed April 1, 2017).

685 [34] R. Prasad, K. Sirkar, Dispersion-free solvent extraction with microporous hollow
686 fiber modules, AIChE J. 34 (1988) 177–188.

687 [35] L. Dahuron, L. Cussler, Protein Extractions with Hollow Fibers, AIChE J. 34
688 (1988) 131–136. doi:10.1002/aic.690340115.

689 [36] E. Drioli, A. Criscuoli, E. Curcio, Membrane contactors:Fundamentals,
690 applications and potentialities., in: Membr. Sci. Technol. Ser. vol.11, Amsterdam,
691 2006.

692 [37] Y. Cengel, M. Boles, Thermodynamics:An Engineering Approach, 6th ed.,
693 McGraw-Hill, New York, 2008.

694 [38] X. Shi, G. Tal, N.P. Hankins, V. Gitis, Fouling and cleaning of ultrafiltration
695 membranes: A review, J. Water Process Eng. 1 (2014) 121–138.
696 doi:10.1016/j.jwpe.2014.04.003.

697 [39] H. Lin, W. Peng, M. Zhang, J. Chen, H. Hong, Y. Zhang, A review on anaerobic
698 membrane bioreactors: Applications, membrane fouling and future perspectives,
699 Desalination. 314 (2013) 169–188. doi:10.1016/j.desal.2013.01.019.

700 [40] J. Zhang, S.I. Padmasiri, M. Fitch, B. Norddahl, L. Raskin, E. Morgenroth,
701 Influence of cleaning frequency and membrane history on fouling in an
702 anaerobic membrane bioreactor, Desalination. 207 (2007) 153–166.
703 doi:10.1016/j.desal.2006.07.009.

704 [41] M.H. Al-Malack, M.M. Rahman, Treatment of refinery wastewater using mebrane
705 processes, in: K. Mohanty and M.K. Purkait (Eds.), Membrane technologies and
706 applications, CRC Press, Boca Raton, USA, 2012, pp 121–132.